Chapter 15

Side-Path Electron Donors: Cytochrome b_{559}, Chlorophyll Z and β-Carotene

Peter Faller*, Christian Fufezan and A. William Rutherford*
Service de Bioénergétique, Département de Biologie Joliot-Curie, CNRS URA 2096, CEA Saclay, F-91191 Gif-sur-Yvette, France

*Authors for correspondence, email: faller@lcc-toulouse.fr; [2]rutherford@dsvidf.cea.fr

T. Wydrzynski and K. Satoh (eds): Photosystem II: The Light-Driven Water:Plastoquinone Oxidoreductase, pp. 347–365.

Summary

β-Carotene (Car), cytochrome (Cyt) b_{559} and a monomeric chlorophyll (Chl) designated as chlorophyll Z, all undergo oxidation in Photosystem (PS) II under some illumination conditions. These components are not part of the direct electron transfer that leads to water oxidation and plastoquinone reduction and are thus designated 'side-path electron donors.' Under the usual conditions of PS II function, the quantum yield for the oxidation of these components is low; however, under certain experimental conditions, particularly low temperatures, the dominant reactions can be those involving the side-path donors. Car is a branch point in the side-path electron donation, being oxidized by P^+ (the kinetically competent Chl cation radical), and reduced by Cyt $b_{559,}$ which is itself reduced by electrons from the pool of plastoquinol, possibly through the Q_B site. This all occurs on the D2-side of the reaction center. When the Cyt b_{559} is pre-oxidized, Car^+ is reduced by Chl Z. There are two candidates for Chl Z, the more obvious candidate on the D2 side and the less straightforward candidate on D1 side of the reaction center. The side-pathway is usually rationalized as a photoprotective cycle aimed at removing long-lived P^+ and thus limiting oxidative damage. Based on the low quantum yields, we consider this unlikely. Instead we suggest that the side-path constitutes a photoprotective cycle in which the aim is to reduce the Car cation, rather than P^+, returning the carotene cation to its unoxidized state, preventing adventitious reactions and allowing it to play its a role as a singlet O_2 quencher in the heart of PS II.

I. Introduction

Photosystem II (PS II) is a photochemical enzyme that uses light to drive the reduction of plastoquinone and the oxidation of water. The structure and function of PS II has been extensively reviewed (Goussias et al., 2002; Rappaport and Diner, 2002; Chapters 18–21). Several components have been shown to be oxidized in PS II other than the components directly associated with water oxidation. Cytochrome b_{559} (Cyt b_{559}), a chlorophyll Z (Chl Z), β-carotene (Car) have all been reported as 'side-path' electron donors in PS II. Understanding the side-path donors, their nature, structure, position, how they work and their significance to PS II function are all important for several reasons. First, these species may play roles in the regulation and protection of the reaction center (RC) under physiologically relevant conditions. Second, they constitute a significant proportion of the cofactors in PS II that cannot be ignored in structural terms and they may have as yet undetermined functional roles. Last, and of particular importance, a precise understanding of when and where the reactions of the side-path donors contribute to PS II electron transfer allows them to be clearly distinguished from the processes directly involved in enzyme function, and their influence on the kinetics of enzyme function to be fully understood.

Here we review the side-path electron donor pathway that involves Cyt b_{559}, Chl Z and Car. We deal with some structural aspects of Chl Z and Car, but Cyt b_{559} is only discussed in respect to its involvement in the alternative electron pathway, other aspects are covered elsewhere (Stewart and Brudvig, 1998; Chapter 16, Noguchi and Berthomieu).

Abbreviations: BRC – bacterial reaction center; Car – redox active β-carotene; Car_{D2} – β-carotene associated with D2; $Car_{D2\text{-}43}$ – β-carotene associated with both D2 and CP43; Chl Z – side-path redox-active Chl; Chl – chlorophyll; Chl_{D1}, Chl_{D2} – monomeric Chls that are bound to D1 and D2, respectively; Cyt b_{559} – cytochrome b_{559}; D1, D2 – reaction center core proteins; ENDOR – electron nuclear double resonance; EPR – electron paramagnetic resonance; ESEEM – electron spin echo envelope modulation; FTIR – Fourier transform infrared; HYSCORE – hyperfine sublevel correlation spectroscopy; OEC – oxygen evolving complex; P – central cluster of Chls that comprise the primary electron donor; $P_{D1}P_{D2}$ – two monomeric Chls associated with D1 and D2, respectively, that are counterparts to the special pair Chls in the BRC; PS II – Photosystem II; Q_A, Q_B, – primary and secondary plastoquinone electron acceptors; Y_Z, Y_D – redox-active tyrosines bound to D1 and D2, respectively

II. Location of Accessory Electron Donors

A scheme of the structure of PS II is shown in Fig. 1. This is based on the refined 3.5 Å X-ray diffraction crystal structure (Zouni et al., 2001; Kamiya and Shen, 2003; Ferreira et al., 2004) but is similar in most respects to earlier models that were based on the structure of the purple bacterial reaction center (BRC), comparative spectroscopy, sequence analysis

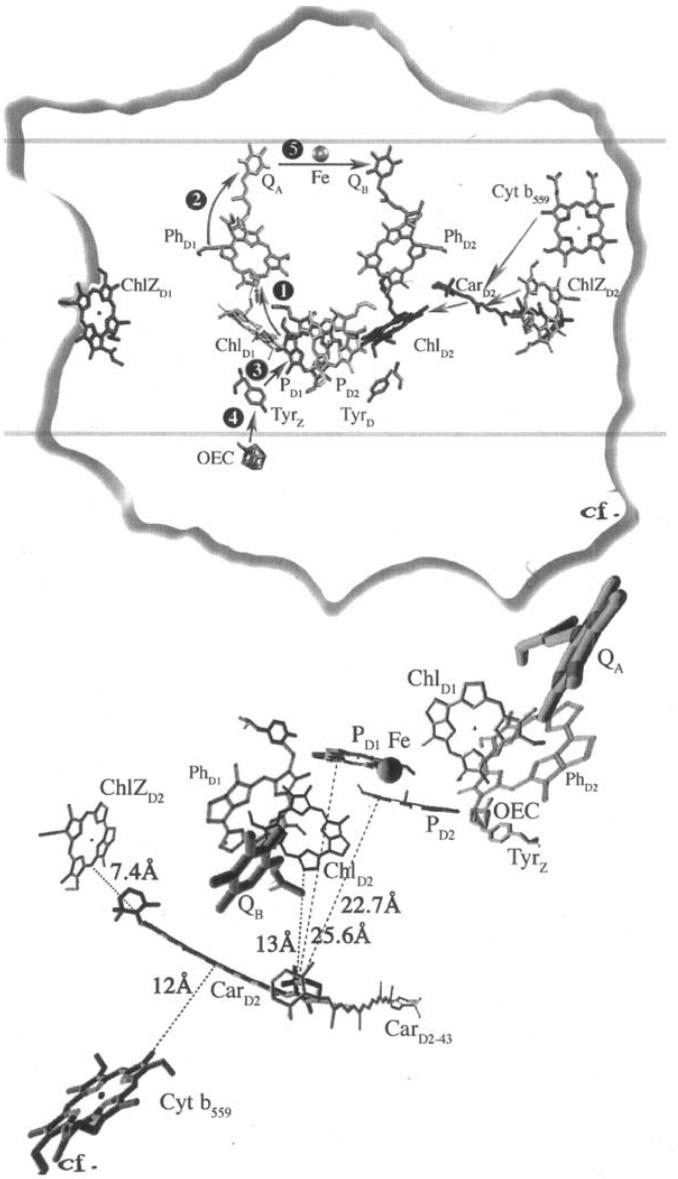

Fig. 1. The upper part shows a structural model of the PS II reaction center showing the arrangement of the cofactors. The electron transfer chain resulting in water oxidation and plastoquinone reduction is marked by numbered arrows. The numbers indicate the order in which the reactions take place. The electron transfer chain from the side-path donors is marked with unnumbered arrows. The cofactors are labeled with abbreviations that are defined in the text but are supposed to be as evident as possible. The boundary of the D1/D2/Cyt b_{559} complex is given as is the approximate position of the membrane. The model is drawn based on the current crystal structure (Ferreira et al., 2004). The lower part shows a view of PS II from above (non-heme iron side) showing the positioning of the carotenes Car_{D2} and Car_{D2-43}, Chl Z_{D2} and Cyt b_{559} relative to the central Chls of PS II. The vectors shown are the shortest distances between Car_{D2} its potential electron transfer partners (including P_{D1} P_{D2} and Chl_{D2}) measured edge to edge from the conjugated parts of the molecules (data from the coordinates from Ferreira et al., 2004).

and folding models, biochemical work, electron diffraction and spectroscopic structural measurements (Rutherford and Faller, 2001).

A. Cytochrome b_{559}

From the early days, the fact that Cyt b_{559} was oxidized at cryogenic temperatures led to the idea that it must be integral to the core of the reaction center (Knaff and Arnon, 1969). This idea was confirmed when the smallest isolated complex that was still capable of charge separation was found to contain only the D1, D2 and Cyt b_{559} (Nanba and Satoh, 1987). From the crystal structure, Cyt b_{559} is located adjacent to the D2 subunit (Zouni et al., 2001).

The number of Cyt b_{559} per PS II has been debated for many years (Stewart and Brudvig, 1998). The first crystal structure of PS II from cyanobacteria showed the presence of only one Cyt b_{559} (Zouni et al., 2001). One might have expected this to end the debate. However, Zouni et al. (2001) raised the possibility that a second cytochrome could have been lost during the preparation. The symmetry-related location on the D1-side indeed contains two *trans*-membrane helices like those of the cytochrome but there is no heme. However we consider that the loss of the putative second heme may well have occurred during the evolution rather than the isolation of PS II (for further discussion, see Stewart and Brudvig, 1998; Chapter 16, Noguchi and Berthomieu).

B. Chlorophyll Z

The smallest PS II reaction center preparation contains six Chls, two pheophytins, two β-carotenes and one heme. One or two of the Chls and a β-carotene can be lost when harsher isolation procedures are used (Satoh, 1996). This stoichiometry differs from that in the BRC, which contains four bacterio-Chls (BChls) rather than six. An obvious explanation was that the two additional and easily lost Chls in PS II corresponded to the Chl Z and its symmetrical counterpart that were predicted to be bound to D1-His118 and D2-His117 on the periphery of the complex (Ruffle et al., 1992).

Other evidence for the location of the Chl Z (and its symmetrical counterpart) came from EPR relaxation studies that placed Chl $Z^{+\bullet}$ at a distance of 39.5 Å from the non-heme Fe, a distance that corresponded well to the predicted position of D1-His118 and D2-His117 in the folding model (Koulougliotis et al., 1994). Further strong evidence came from site-directed mutagenesis on the D1-His118 and D2-His117, the supposed ligands of Chl Z_{D1} and Chl Z_{D2}, respectively. These mutants showed changes attributable to Chl Z as measured by resonance Raman (Stewart et al., 1998) and fluorescence quenching (Wang et al., 2002). Given this information, densities attributable to Chl Z were pointed out in both D1 and D2 in the crystallographic models (Zouni et al., 2001). The question of whether the oxidizable Chl Z corresponds to Chl Z_{D1} or Chl Z_{D2} is discussed below.

C. β-Carotene

The observations that carotenoid could be oxidized at liquid helium temperature (Schenck et al., 1982; Hanley et al., 1999) indicated that it must be in the heart of the RC. The isolated D1/D2/Cyt b_{559} complex indeed contained two Car molecules (Satoh, 1996) and these could be oxidized upon illumination under some circumstances (Telfer et al., 1991; Telfer, 2002).

While the first crystal structure of PS II at 3.8 Å assigned densities to the other cofactors as predicted from earlier work, no densities were assigned to the carotenoids (Zouni et al., 2001). The second structure by Kamiya and Shen (2003) at 3.7 Å assigned some density to the carotenoids, placing two Car molecules on D2. Shen revised this model, making the *cis* Car into all *trans*, extending one Car so that it approached the Chl Z_{D2} (Shen and Kamiya, 2003). The first refined crystal structure at 3.5 Å supported this position for the one β-carotene (see Fig. 1) but the second was less closely associated with D2 (Ferreira et al., 2004).

The Car most closely associated with D2 (Car_{D2}) lies approximately parallel to the membrane plane along the outside surface of the D2 and approaches the Chl Z_{D2} (see Fig. 1). As it crosses over the D2 surface, it runs along the interface between D2, the J-subunit and the β-subunit of Cyt b_{559} (Chapter 6, Thornton et al.). One of the head groups of Car_{D2} gets very close (nearest aromatic edge to edge 7.4 Å) to Chl Z_{D2}, while the other head group is only 3.8 Å from the second carotenoid. This Car, which is approximately perpendicular to the membrane plane (and to the Car_{D2}), runs from D2 to the CP43 subunit, and is thus designated here $Car_{D2\text{-}43}$. In addition to its proximity to Car_{D2}, the $Car_{D2\text{-}43}$ runs down the outside of D2, approaching only a few amino acids (notably those of the J, K and D1 subunits), and reaching the

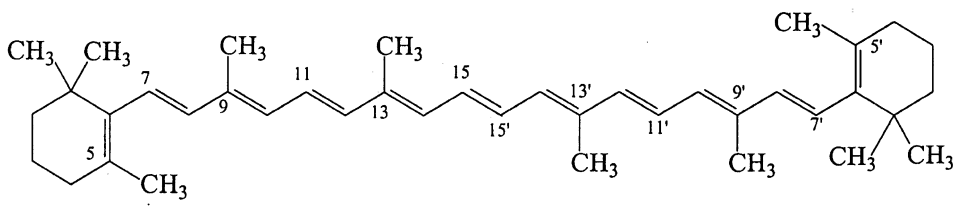

Fig. 2. Chemical structure of β-carotene.

lumenal side antenna Chls of CP43. Intriguingly, on the way it rubs up against the isoprene tails of the Chl_{D2} and Q_B near the surface of D2. It also approaches (to within 8.7 Å) a third carotenoid that is mainly associated with the K subunit (see Ferreira et al., 2004).

Seven carotenoids were modeled into the crystal structure of PS II, which fits reasonably well to the estimated number based on extraction of pigments from the complex (J. Barber, personal communication; however, see Tracewell et al. (2001b) who reported more than twice this number in *Synechocystis*). In addition to the three carotenoids mentioned above, the remaining four are arranged in two pairs, one pair on the outer surface of CP43 and another in a similar location on CP47, both well away from potential side-path action. It seems quite possible that the two Car molecules associated with the isolated D1/D2/Cyt b_{559} correspond to the Car_{D2} and $Car_{D2\text{-}43}$, described above, with the Car_{D2} being held in place by the cytochrome subunit and $Car_{D2\text{-}43}$ being attached to the first Car but more loosely bound to the exterior of D1/D2.

The location of the Car_{D2} in the crystal structure (Fig. 1) corresponds in general terms to the predictions for the redox active carotenoid from spectroscopic work, in that it is located between the central pigments, the Cyt b_{559} and the Chl Z (Hanley et al., 1999). Other more specific suggestions based on spectroscopy appear less successful: (i) The electron spin echo modulation (ESEEM) identification of a close interaction between $Car^{+\bullet}$ and a tryptophan nitrogen nucleus led Deligiannakis et al. (2000) to identify a group of conserved tryptophans in D2 as the likely site for the Car. The crystal structure shows that these tryptophans do not constitute the site (Ferreira et al., 2004). Indeed there are no appropriately located tryptophans close to either Car_{D2} or $Car_{D2\text{-}43}$ in the structure. An alternative candidate for the nitrogen coupling is not yet clear; however, the close association with the Chl Z_{D2} raises the possibility that a tetrapyrrol nitrogen could be involved. (ii) The dipolar 38 Å distance from the non-heme iron to $Car^{+\bullet}$ deduced from a saturation recovery method (Lakshmi et al., 2003) corresponds poorly with the crystal structure. Considerations of the spin distribution led the authors to place the $Car^{+\bullet}$ on the luminal side of the reaction center with the nearest part of the molecule at 38 Å: far from the actual location (the nearest part of the $Car^{+\bullet}$ to the Fe is 28 Å). The discrepancy could be due to an unexpected localization of the spin on the $Car^{+\bullet}$ or to technical problems such overlap from the Chl $Z^{+\bullet}$ signals (see also the next paragraph). (iii) Tracewell and Brudvig (2003) observed the apparent influence of the redox state of Y_D on the absorption spectrum of the $Car^{+\bullet}$. This was attributed to an electrostatic effect of $Y_D^{\bullet}(H^+)$on the closer of the two carotenoids. The proximity of the Car to the Y_D and the model deduced from that work fits poorly with the crystal structure. However the effect is worth reinvestigating in the light of the new structural model.

The current crystal structure contradicts models in which the two Car molecules were positioned symmetrically in both D1 and D2 (Faller et al., 2001a; Tracewell et al., 2001a,b; Lakshmi et al., 2003; Telfer, 2002). In these cases the models were not based on spectroscopic evidence for a D1 side Car, but rather on the extension of the cofactor symmetry in the reaction center. In fact, for carotenoids, the BRC, which has provided the basis for models of PS II for decades, did not exhibit such symmetry for the location of the carotenoid (Michel and Deisenhofer, 1988), and the current crystal structure of PS II is like the BRC in that respect (Ferreira et al., 2004).

Having listed the apparent mismatches between the crystal structure and the spectroscopic models, it is worth making the following points. The crystal structure has a resolution of 3.5 Å and precedence indicates that at this resolution carotenoids are among the more difficult cofactors to fit due to their similarities with isoprene tails and lipids. Thus, some

changes in the precise location of the carotenoids might be expected as the crystal structure improves. Secondly, the structure raises the possibility that electron transfer between adjacent carotenoids could allow the cation to migrate out away from D2 into the peripheral antenna under some conditions. This could mean that the spectroscopists are measuring a carotene cation different from $Car_{D2}^{+\bullet}$, at least under some experimental conditions.

III. Spectroscopic Studies

A. β-Carotene

1. Neutral Carotenes

Spectroscopic and biochemical analyses showed that two Car molecules were present in the D1/D2/Cyt b_{559} complex. There is still some debate concerning their *cis* or *trans* configuration (Telfer, 2002). Isolation studies gave conflicting results (Bialek-Bylka et al., 1995; Yruela et al., 1998). The majority of the spectroscopic studies assumed that both are in the *trans* configuration (Tracewell et al., 2001b; Telfer, 2002). The recent crystallographic model of Kamiya and Shen (2003) suggested that one of the Cars was in a *cis* conformation, but this model was later revised to both being all-*trans* (Shen, 2003). The refined crystal structure shows only one (all *trans*) β-carotene (Car_{D2}) within D1/D2 and that is located in D2 (Ferreira et al., 2004). A second (all *trans*) β-carotene runs from D2 to CP43 (Car_{D2-43}) and approaches (3.8 Å) the Car_{D2}. We suggested above that the second Car co-isolated with D1/D2/Cyt b_{559} complexes could be Car_{D2-43}, stuck to the outside of the complex.

Linear dichroism measurements on D1/D2/Cyt b_{559} complex preparations showed a positive and a negative peak that was interpreted either as arising from excitonic interactions between the two Car molecules (i.e., proximity) or reflecting the presence of two distinct Car molecules (Van Dorssen et al., 1987a; Renge et al., 1996; Germano et al., 2001; for recent reviews see Tracewell et al., 2001b; Telfer, 2002). The most recent data is interpreted as a two strongly coupled carotenoids (Frese et al., 2003). Similarly several studies indicate a different orientation of the dipole moment of the two transitions, indicating a different orientation for the two neutral carotenoids (van Dorssen et al., 1987b; Breton et al., 1988; Kwa et al., 1992; Tomo et al., 1997). The carotenoid with absorption transitions at 507/473/443nm is nearly parallel to the membrane while the 489/458/429nm carotenoid is closer to 45° to the membrane but approximately perpendicular to the other carotenoid. These data appear to be consistent with the idea that the two β-carotenes in D1/D2/Cyt b_{559} complexes correspond to Car_{D2} and Car_{D2-43} in the most recent crystal structure, at least within the limits of the resolution of that model. The Car moleucles are close enough to be coupled and they appear to be all-*trans* and oriented at approximately right angles to each other (Ferreira et al., 2004). The Car with absorption transitions at 507/473/443nm (Car_{507}) would then correspond to the Car_{D2}, while the 489/458/429nm carotene (Car_{489}) would correspond to Car_{D2-43}. The latter is expected to be more exposed to solvent and detergent, so is more likely to exhibit variability its spectroscopic and chemical properties in isolated D1/D2/Cyt b_{559} complexes.

2. Electronic Absorption of the β-Carotene Cation Radical

The $Car^{+\bullet}$ in PS II shows a strong absorbance band at about 990 nm in spinach and *Synechocystis* with an extinction coefficient of about 160,000 (Hanley et al. 1999, Tracewell et al., 2001a). A shoulder around 880 nm was also assigned to $Car^{+\bullet}$ (Faller et al., 2001a; Tracewell et al., 2001a). The position at 990 nm is typical for β-carotene cation radical as reported in in vitro experiments (Mathis and Vermeglio, 1972; Dawe and Land, 1975; Moore et al., 1984; Edge et al., 2000). It is also distinct from the doubly oxidized β-carotene cation that absorbs at around 800 nm (Jeevarajan et al., 1996a). Tracewell et al. (2003) deconvoluted the $Car^{+\bullet}$ spectrum in a range of experimental conditions and concluded that two different $Car^{+\bullet}$ species exist. Given the most recent model where two Car molecules are in close proximity and a third is fairly close (Ferreira et al., 2004), it seems possible that the two spectra represent different environments that perturb the charge distribution over the two or more carotenoids under different experimental conditions.

3. Electron Magnetic Resonance Studies

The $Car^{+\bullet}$ shows an X-band electron paramagnetic resonance (EPR) signal at g = 2.0025 ± 0.0001 and line-width about 10.5 ±1 G (Hanley et al., 1999; Faller et al., 2001a). These values are similar to $Car^{+\bullet}$ generated in vitro and typical for organic radicals

in general (Grant et al., 1988). Faller et al. (2000) and Lakshmi et al. (2000) measured high field EPR of $Car^{+\bullet}$ in PS II in spinach and *Synechocystis*, respectively. The g-values reported agreed quite well (spinach/*Synechocystis*:g_x 2.00322/35, g_y 2.00252/1, g_z 2000211/27). These g-values are clearly distinct from the g-values obtained from the canthaxanthin cation radical (a carotenoid having two ketogroups at position 4, see Fig. 2), generated in vitro (on silica-alumina surface). The $Car^{+\bullet}$ in PS II has a rhombic g-tensor, while the g-value of the canthaxanthin cation radical on the silica-alumina surface is axial (Konovalova et al., 1999). The origin of this difference is not clear yet, but the different environment between the protein matrix and the silica-alumina surface could be responsible, rather than the influence of the two keto groups (Faller et al., 2000; see below). Indeed it is possible that the carotenoid on the silica-alumina surface has undergone significant chemical changes.

ESEEM and hyperfine sublevel correlation spectroscopy (HYSCORE) measurements were interpreted as showing that $Car^{+\bullet}$ in PS II interacts with an indol nitrogen from a tryptophan in its vicinity (Deligiannakis et al., 2000). The Car_{D2} in the recent crystal structure (Ferreira et al., 2004) does not approach any such tryptophan. How can this be explained? Three possibilities arise: (i) The assignment could be wrong (perhaps the pyrrol nitrogen of the neighboring Chl Z_{D2} is responsible for the ^{14}N couplings). (ii) As a result of electron transfer, the cation could be on a different carotenoid, however, a preliminary hunt shows that the more peripheral carotenoids do not approach any tryptophan groups either; the nearest appears to be Trp271 of D1 at around 6 Å. (iii) The crystal structure at the level of the carotene may be wrong or, as they say in the trade: 'it may yet undergo further refinement.'

The β-carotene cation radical generated on silica-alumina showed an interaction with an Al nucleus (Konovalova et al., 2001). The ENDOR measurement of $Car^{+\bullet}$ in PS II showed the largest hyperfine splitting in the range of ~8 MHz suggesting that the spin is delocalized over the Car molecule. Comparable hyperfine splittings were obtained from β-carotene cation radical formed by oxidation with iodine in organic solvent (Faller et al., 2001). These observed hyperfine splitting values were confirmed recently by a density functional theory study of Himo (2001). This study suggested a spin delocalization over the entire π-conjugated system including the double bonds in the head groups (see Fig. 2).

Electron nuclear double spin (ENDOR) measurement of the β-carotene cation radical and two other carotenoid radical cations (canthaxantincation radical and 8′-apo-β-caroten-8′-al) on a silica alumina solid supports exhibited high hyperfine splitting values of about 13 MHz (Jeevarajan et al., 1993). Based on semi-empirical INDO-type calculations, this was assigned to the methyl groups at position 13 and 13′ (see Fig. 2). This indicated a higher spin concentration in the middle of the molecule compared to the measurement mentioned above. These differences could again be due to interaction with the support (Faller et al., 2000; Himo, 2001) or to different conformations (Konovalova et al., 2001)

4. Vibrational Spectroscopy

Fourier transform infrared (FTIR) spectroscopy of β-carotene cation radical in PS II and organic solvents (oxidized by iodine) was reported by Noguchi et al. (1994). Bands at 1465, 1441, 1148, 992 and 966 cm^{-1} were assigned to $Car^{+\bullet}$ in PS II, which were partly comparable to the β-carotene cation radical in organic solvents (1479, 1151 and 1001 cm^{-1}). The authors pointed out that the structure of β-carotene cation radical in PS II and organic solvents differ somewhat, but no details or possible reason was given or discussed.

Raman measurements of $Car^{+\bullet}$ in D1/D2/Cyt b_{559} complexes and PS II membranes have been reported (Pascal et al., 1999; Vrettos et al., 1999; Telfer et al., 2003). The most intense bands were very similar in the different studies and were located around 1001, 1154, 1484 and 1525 cm^{-1}. The spectra of $Car^{+\bullet}$ in D1/D2/Cyt b_{559} complexes and PS II membranes were in agreement with a slightly twisted all-*trans* conformation of the $Car^{+\bullet}$(A. Pascal, personal communication). The most recent study attributed vibrational bands at 1485 and 1525 cm^{-1} to the Car_{507} and bands at 1491 and 1537 cm^{-1} to a Car_{489} cation (Telfer et al., 2003). Based on the orientation data described above and the crystal structure (Ferreira et al., 2004), we might assign these to the Car_{D2} (Car_{507}) and the $Car_{D2\text{-}43}$ (Car_{489}) in the crystal structure. The legitimacy of these assignments will be tested by future refinements of the crystal structure.

Jeevarajan et al. (1996b) reported that the extent of the downshift of the v1 frequency (around 1530 cm^{-1}) in going from neutral carotenoids to the radical cation depends on the length of the conjugated chain.

By applying this hypothesis to the $Car^{+\bullet}$ in D1/D2/Cyt b_{559} complex, a more localized spin distribution, i.e., not over the entire conjugated chain, was suggested (Pascal et al., 1999). However, this was contradicted by the EPR measurements as well as the density functional theory study (Faller et al., 2000, 2001b; Himo, 2002).

The resonance Raman spectrum of $Car^{+\bullet}$ in intact (water oxidizing) and Mn-depleted PS II showed no significant differences. In contrast, minor differences were observed when it was compared to $Car^{+\bullet}$ in D1/D2/Cyt b_{559} preparations indicating that latter preparation affects the structure pigments (A. Pascal, personal communication). This fits with the crystal structure which shows that the carotenes are predicted to be exposed in D1/D2/Cyt b_{559} preparations.

B. The Active Chlorophyll Z Cation Radical

The realization that $Car^{+\bullet}$ can accumulate in the majority of the centers by illumination at temperatures lower than 77K raised questions about many earlier studies done under such conditions where it had been assumed that only Chl $Z^{+\bullet}$ was present. It seems likely that such studies would have been at least contaminated with $Car^{+\bullet}$ (see above and Hanley at al., 1999; Vrettos et al., 1999). This holds in particular for (X-band) EPR studies where $Car^{+\bullet}$ and $Chl^{+\bullet}$ show almost identical spectra (see below) but this may also have been a problem in other kinds of spectroscopic studies.

1. Electron Magnetic Resonance Studies

Chl $Z^{+\bullet}$ shows an X-band EPR signal at g=2.0025 ±0.0001 and a line width of about 10.5 ±1 G (Visser et al., 1977; DePaula et al., 1985; Hanley et al., 1999). These values are similar to $Car^{+\bullet}$ generated in PS II and therefore virtually indistinguishable. They were distinguished originally by matching optical absorption studies (Hanley et al., 1999); and subsequently by using more sophisticated EPR methods. High-field EPR of Chl $Z^{+\bullet}$ was measured in spinach and *Synechocystis*: (MacMillan et al., 1998; Faller et al., 2000; Lakshmi et al., 2000). The two studies of spinach PS II showed essentially identical g-values (e.g., g_x 2.00308, g_y 2.00253, g_z 2.00216), whereas Chl $Z^{+\bullet}$ from *S. lividus* exhibited a higher g-anisotropy (g_x-g_z = 11.0) and a very low g_z value (g_x 2.00312, g_y 2.00263, g_z 2.00202). This remains unexplained. The spectrum of Chl $Z^{+\bullet}$ at high field is also somewhat different from $Chl^{+\bullet}$ generated in organic solvent, probably reflecting the different environment (Bratt et al., 2000; Un et al., 2001).

ESEEM was measured on Chl $Z^{+\bullet}$ by Deligannakis et al. (2000) and a spectrum dominated by features originating from the pyrol ^{14}N nuclei were reported. Also ENDOR measurements of Chl $Z^{+\bullet}$ revealed similar hyperfine couplings to those seen for $Chl^{+\bullet}$ in organic solvents (Lubitz, 1991; Rigby et al., 1994; Faller et al., 2001b). In the pulsed ENDOR study of Chl $Z^{+\bullet}$, two hyperfine couplings at 10.8 and 14.9 MHz were detected and assigned to the β-H at position 17 and 18 (Fig. 3). In contrast, $Chl^{+\bullet}$ in organic solvent exhibited only one broad hyperfine coupling at 12.5MHz. Hence it appears that the protein imposes a distinct conformation, leading to two distinct and resolved hyperfine couplings in Chl $Z^{+\bullet}$ (Faller et al., 2001b).

2. Vibrational Spectroscopy

FTIR difference spectrum of Chl $Z^{+\bullet}$/Chl Z exhibited positive bands at around 1747 and 1714 cm^{-1}, which were assigned to the carboxy C=O and keto C=O, respectively (Fig. 3) (Noguchi et al., 1994; Noguchi and Inoue, 1995). Again the spectrum was similar to $Chl^{+\bullet}$/Chl in organic solvent. Resonance Raman on Chl $Z^{+\bullet}$ was reported by Cua et al. (1998). Since the illumination was given at 30K it seems likely that some $Car^{+\bullet}$ was also formed and probably contributed significantly to the spectrum (the $Car^{+\bullet}$ electronic absorption spectrum tales down to the absorption of Chl $Z^{+\bullet}$). It seems that most of the bands detected in the $Car^{+\bullet}$ spectrum were also present in the Chl $Z^{+\bullet}$ spectrum. Also the most prominent band around 1480 cm^{-1} of Chl $Z^{+\bullet}$ has a corresponding band in $Car^{+\bullet}$, i.e., at 1484 cm^{-1}, which is also one of the most intense bands (Vrettos et al., 1999; Pascal et al., 1999; Telfer et al., 2003). This is supported by FTIR, where both, Chl $Z^{+\bullet}$ and $Car^{+\bullet}$, exhibited a band around 1480 cm^{-1}. Thus, the designation of the band around 1480 cm^{-1} as a benchmark for Chl $Z^{+\bullet}$ (Tracewell et al., 2001a) is questionable (Telfer et al., 2003).

3. Orientation

Information concerning the angular orientation of Chl $Z^{+\bullet}$ with respect to the membrane has been obtained from one-dimensional oriented PS II membranes by high-field EPR measurements (Faller et al., 2000). Assuming a similar orientation of the g-tensor in

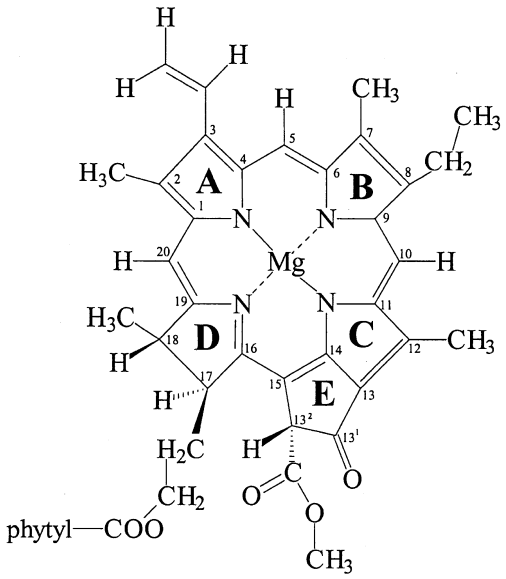

Fig. 3. Chemical structure of chlorophyll *a*.

Chl $Z^{+\bullet}$ as for BChl $a^{+\bullet}$, the ring plane of the Chl $Z^{+\bullet}$ was found to be oriented perpendicular to the membrane plane. This is consistent with the orientation of both Chls assigned to Chl Z_{D1} and Chl Z_{D2} in the current model from crystallography shown in Fig. 1 (Zouni et al., 2001; Ferreira et al., 2003).

IV. Electron Transfer Pathways

A. The Mainline Electron Transfer Pathway

A few hundred picoseconds after the absorption of a photon by PS II the radical pair formed consists $P^{+\bullet}/Q_A^{-\bullet}$ (electron transfer reactions shown as arrows 1 and 2 in Fig. 1), where $P^{+\bullet}$ is a Chl cation radical located on one or the other (through a redox equilibration) of the two Chl monomers (P_{D1} and P_{D2}) and $Q_A^{-\bullet}$ is a plastosemiquinone (reviewed in Rappaport and Diner 2002; Chapter 7, Renger and Holzwarth). Tyrosine 161 of D1 (Y_Z) acts as an electron donor to $P_{D1}^{+\bullet}$ (arrow 3 in Fig. 1) and the $Y_Z^{+\bullet}$ oxidizes the Mn cluster in the first step of the redox cycle required for water oxidation (arrow 4 in Fig. 1). In the majority of centers donation from Y_Z to P_{D1} is rapid and efficient in out-competing the charge recombination reaction $P^{+\bullet}/Q_A^{-\bullet}$ to PQ_A. In some centers Y_Z donation is slower, reflecting heterogeneities, perhaps associated with pKs on groups affecting, for example, the de-protonation of the tyrosine, the location of the $P^{+\bullet}$ cation and the redox potentials of these cofactors. On each state in the enzyme cycle the rates of donation vary depending on accumulated charges, movements of charged species (protons, and possibly Cl^-) and structural changes. As a result $P^{+\bullet}$ is relatively long-lived in a statistical fraction of center during enzyme function. In centers where the OEC is dysfunctional or absent (e.g., prior to or during assembly of the Mn cluster) then long-lived $P^{+\bullet}$ is expected to occur on the majority of charge separations.

When electron donation to $P^{+\bullet}$ is slow, and consequently $P^{+\bullet}$ long-lived, the back-reaction from $Q_A^{-\bullet}$ will occur (200 μs^{-1} ms) (for a review, see Rappaport and Diner, 2002). This reaction will be in competition with electron transfer from $Q_A^{-\bullet}$ to Q_B (or $Q_B^{-\bullet}$) (arrow 5 in Fig. 1). Thus in some centers the lifetime of P^+ could be significantly longer than the $P^{+\bullet}/Q_A^{-\bullet}$ radical pair recombination lifetime. Prior to photoactivation Q_A has a higher potential and this decreases the efficiency $Q_A^{-\bullet}$ to Q_B electron transfer and may limit the long-lived $P^{+\bullet}$ as well as affecting the charge recombination route (Johnson et al., 1995).

$P^{+\bullet}$ is the most oxidizing species in PS II with an estimated potential of around 1.1 V or higher (Rappaport and Diner, 2002; Rutherford and Faller, 2002). It is potentially capable of oxidizing cofactors or amino acid side chains in its vicinity other than the those directly involved in the water-plastoquinone oxidoreductase activity. The side-path electron donations (arrows from the right in Fig. 1) are generally considered to function as redox quenchers of $P^{+\bullet}$, limiting unwanted and potentially damaging side-reactions. Given the high yields of water oxidation, the yields of oxidation of the side-path donors are expected to be very low; however, the yields are liable to increase under any of the conditions where the lifetime of $P^{+\bullet}$ increases.

B. Side-Path Electron Donors: Historical Summary

The oxidation of Cyt b_{559} upon illumination has been known and studied for many years (Stewart and Brudvig, 1998). In intact PS II this occurs in the majority of the centers with a low quantum yield when illumination is given at 77K or below. In some centers a high quantum yield electron donation probably from Y_Z, can take place, forming the $Y_Z^{+\bullet}$ $Q_A^{-\bullet}$ state,

at least when in the S_0 and S_1 states (Nugent et al., 2002; Zhang and Styring, 2003; C. Zhang and A.W. Rutherford, unpublished). At temperatures where the Mn oxidation can take place (around 200K or higher, depending on the S-state), Cyt b_{559} oxidation is greatly out competed (Mathis and Vermeglio, 1975; DePaula et al., 1985). At physiological temperatures a small fraction of the cytochrome seems to go oxidized through the redox equilibration of the oxidizing equivalent in the S_2 and S_3 redox states of the OEC (Buser et al., 1992).

If Cyt b_{559} is preoxidized, Chl $Z^{+\bullet}$ is generated instead with similar yields (Visser et al., 1977; Thompson and Brudvig, 1988). This turns out to be the most common situation in PS II preparations where the electron donor side is modified, damaged or where the Mn complex is absent. The redox potential of the cytochrome is extremely sensitive to mistreatment and shifts from the (usually) native high potential form to the low potential form resulting in the oxidation of the heme under ambient redox conditions (Stewart and Brudvig, 1998). However, when the Cyt b_{559} is reduced in Mn-depleted PS II it can be oxidized with a low quantum yield upon illumination at all temperatures below that where Y_Z donation is inhibited (lower than around –30 °C) (Faller et al., 2001a).

Carotenoid cation photogeneration was observed first when lipophilic redox reagents were added to PS II (Velthuys, 1981; Schenck et al., 1982) but early on it was recognized that the presence of these chemicals was not required under some conditions (Schenck et al., 1982). For many years its sub-stoichiometry and the involvement of the lipophilic anion in most studies, cast carotenoid oxidation as a merely interesting chemical quirk and a redox role for carotenoid in PS II chemistry was rarely considered. This view changed in recent years and it is now thought that β-carotene acts as an electron donor to $P^{+\bullet}$ and is reduced by the Chl Z and Cyt b_{559} (Hanley et al., 1999). In what follows we deal with some of the data and arguments that have contributed to the current understanding of the electron transfer pathway involving Cyt b_{559}, Chl Z and Car.

C. The Alternate Electron Transfer Pathway

The pathway of the alternative donors was addressed by Thompson and Brudvig (1988), considering only Cyt b_{559} and Chl Z, since at that time Car was not recognized as a relevant player. In this work the ability of either Cyt b_{559} or Chl Z to compete with the electron donation of the Mn-cluster/Y_Z was measured. It was assumed that Mn-cluster/Y_Z donation rate gradually decelerated upon lowering the temperature and hence at a given temperature the side-path donors start to compete with the Mn-cluster/Y_Z donation, eventually becoming the dominant donors. This implies that at the temperature where 50% of the side-path donor and 50% Mn-cluster/Y_Z were oxidized upon illumination, the donation rates by the two competing pathways are equal. This experiment was done by: (i) measuring photo-generation of oxidized Cyt b_{559} (i.e., with Cyt b_{559} reduced prior to illumination); and (ii) measuring photo-generation of Chl $Z^{+\bullet}$ (i.e., when Cyt b_{559} was oxidized prior to illumination). It was found that Cyt b_{559} oxidation and Chl Z oxidation showed identical temperature dependencies; thus, it was concluded that the electron donation reaction competing with Y_Z and Mn oxidation was identical for the oxidation of Cyt b_{559} and for Chl Z. The simplest explanation for these observations was a linear electron donation pathway Cyt $b_{559} \rightarrow$ Chl Z $\rightarrow P^{+\bullet}$ (Thompson and Brudvig, 1988).

More recent data indicate that the kinetic model behind these experiments should be revised. Flash kinetic studies by E. Schlodder and H. Derr (personal communication) showed that Y_Z electron donation does not gradually slow down allowing the side-path donors to take over. In fact Y_Z electron donation to $P^{+\bullet}$ only decelerated from a rate of $t_{½}$ = 20 ns at 300 K to $t_{½}$ = 4.2 µs at 150 K. The slower Y_Z electron donation to $P^{+\bullet}$ ($t_{½}$ = 4.2µs) is gradually replaced by the 2ms phase of the $P^{+\bullet}/Q_A^{-\bullet}$ recombination as the temperature is lowered. The rate of oxidation of the side-path donors ($t_{½}$ 20 ms, depending on temperature) remains much slower than this and occurs with a low quantum yield (Hillmann and Schlodder, 1997; Faller et al., 2001a; R. Edge, P. Faller and A.W. Rutherford, unpublished).

A re-interpretation of the Thompson and Brudvig experiment is as follows: The point where Y_Z and the side-pathway become oxidized to an equal extent is not due to a direct competition between two donors with similar rates. Rather, it is due to a cooling-induced heterogeneity of the centers, where in half of the centers Y_Z is oxidized with $t_{½}$ = 4.2 µs while in the other half Y_Z oxidation does not take place and $P^{+\bullet}/Q_A^{-\bullet}$, recombination occurs instead ($t_{½} \sim$ 2 ms). In these centers the continuous illumination results in the photo-accumulation of oxidized electron donors of the side-path with a low quantum yield.

This situation may be complicated further if in

some centers Y_Z donation remains rapid (Nugent et al., 2002; Zhang and Styring, 2003; Zhang et al., 2004) and if in other centers the 'switching off' of Y_Z donation occurs in stages as the temperature is lowered, allowing a low quantum yield donation from Y_Z, in competition with the side-path donors prior to switching off altogether as the temperature is lowered.

The discovery that formation of $Car^{+\bullet}$ upon illumination at low temperature in greater yields than was previously reported, raised the question of where the Car fits in the electron side-pathway and a range of possibilities were considered (Hillman and Schlodder, 1997; Hanley et al., 1999; Vrettos et al., 1999). The observation of Hanley et al. (1999) that the near stoichiometric formation of $Car^{+\bullet}$ upon illumination at 20K was replaced by Chl $Z^{+\bullet}$ when warmed in the dark to temperatures above 77K, led to the suggestion that the following pathway was present:

$$\text{Chl Z} \rightarrow \text{Car} \rightarrow P^{+\bullet}$$

Further support for this arrangement came from the observation that $Car^{+\bullet}/Q_A^{-\bullet}$ recombination could occur at low temperature in competition with the electron donation reaction from Chl Z (Hanley et al., 1999). Similarly Tracewell et al. (2001a) also showed that the recombination of $Car^{+\bullet}/Q_A^{-\bullet}$ was faster than Chl $Z^{+\bullet}/Q_A^{-\bullet}$. Both observations imply a closer localization of Car than Chl Z relative to P.

Hanley et al. (1999) showed that Cyt b_{559} could be oxidized at 20K despite the fact that Chl Z → Car donation was blocked at this temperature in the majority of centers. This led them to favor a branched pathway over the simple linear pathway:

$$\begin{array}{l} \text{Cyt } b_{559} \rightarrow \text{Car} \rightarrow P^{+\bullet} \\ \qquad\qquad\quad \uparrow \\ \qquad\qquad\quad \text{Chl Z} \end{array}$$

It is important to note that while this contradicted the earlier model of Thompson and Brudvig (1988), it did not contradict their data nor their primary conclusion, i.e., that Cyt b_{559} oxidation and Chl Z oxidation were both dependant on the same electron donation reaction to P^+, a reaction that was favored as electron donation from Y_Z was inhibited by lowering the temperature.

Subsequent studies on electron donation rates and yields of the alternative donors also favored this so-called branched pathway and specifically argued against other possible pathways that had been raised earlier (Faller et al., 2001a). The branched pathway (Hanley et al., 1999) was later corroborated by the X-ray crystallographic model (Zouni et al., 2001), which indicated that the edge-to-edge distances between either cofactor (Cyt b_{559} and Chl Z) to the central Chls was more than 35 Å and 25 Å, respectively. Even the shorter Chl Z distance allows only a slow electron transfer rate (~1 s^{-1} according to Page et al., 1999), nearly three orders of magnitude slower than the observed rates. Furthermore the distance between the Cyt b_{559} and the Chl Z was found to be about 24 Å, indicating that direct electron transfer between the cofactors would be very slow. Thus, the Car as an intermediate in the electron transfer as proposed in the branched pathway (Hanley et al., 1999), is required to explain the electron donation rates from Cyt b_{559} and Chl Z to $P^{+\bullet}$. The recent assignment of density to Car in D2 in the crystallographic model supports the branched pathway (Kamya and Shen, 2003; Ferreira et al., 2004; see section III and Figs. 1a and b).

The estimated $t_{½}$ for Car oxidation of 1–2 ms at room temperature (Telfer et al., 1991; R. Edge, P. Faller and A.W. Rutherford, unpublished) is faster than the maximal rate for the 22.7Å distance (i.e., $t_{½}$ = 29 ms, based on Page et al., 1999) between Car and the cation-bearing Chl P_{D1} (note the 25.6 Å distance between Car_{D2} to P_{D2}) (Ferreira et al., 2004; Fig. 2). It thus seems likely that donation occurs via an intermediate cofactor with Chl_{D2} being the likely candidate. The shortest distance between the Car_{D2} and the Chl_{D2} is around 13.1 Å, a distance that would allow a maximum electron transfer rate with a half-time of around 50 nanoseconds (Page et al., 1999). Thus even a very small fraction of the cation on the Chl_{D2}, through an equilibrium with the P Chls, would allow the appropriate kinetics of Car oxidation. Fig. 1 then shows Car_{D2} donating to $P^{+\bullet}$ via Chl_{D2} as the most likely pathway.

The shortest distance between Cyt b_{559} and Car_{D2} is 12 Å units, this corresponds to a maximum rate in the tens of nanoseconds time-scale (Page et al., 1999), in accordance with Cyt b_{559} oxidation being rate-limited by Car_{D2} oxidation (Faller et al., 2001a). Even with the Car_{D2} being closer to both the $Car_{D2\text{-}43}$ and to the Chl Z_{D2} than the Cyt b_{559}, the much lower potential of the cytochrome ensures that it out-competes $Car_{D2\text{-}43}$ and Chl Z as the final location of positive charge-equivalent.

The oxidized Cyt b_{559} can be reduced by electrons from the electron acceptor side. The rate for this reaction is very slow in PS II membranes, being pH-dependent and occurring in the time-scale of many seconds (Buser et al., 1992). In thylakoids, however, in which Q_B functions normally, the rate appears faster ($t_{½}$ = 100 ms) (Whitmarsh and Cramer, 1977). The reaction is inhibited by DCMU and this and the pH dependence of the reaction led Buser et al. (1992) to suggest that electron donor to the oxidized cytochrome is Q_BH_2. In this way the side path connects to the main-line of electron transfer completing a cycle that short-circuits normal electron transfer.

The Q_B head group is 26 Å units from the Cyt b_{559}. This corresponds to a maximal donation rate of around 2.7s much slower than the 100ms rate seen in chloroplasts. There are several possible explanations for this, among which are the following: (i) The electron donation in chloroplasts may not be from Q_BH_2 but from by PQH_2 directly from the membrane side. Indeed the crystal structure shows that the heme is relatively exposed to the membrane. (ii) Another possibility is that electron donation from Q_BH_2 does not occur from the Q_B site but a position closer to the heme as it leaves the site. If we assume that the hydroquinone backs out the way quinone came in, then the position of isoprene chain may represent an entry/exit channel. The quinone's tail gets to within 12 Å of the heme on its way to an obvious channel that connects to the membrane. At this position the Q_BH_2 donation to the heme would be a much more kinetically favorable reaction. The observation that that DCMU inhibits Cyt b_{559} reduction at a lower concentrations than Q_B reduction, implies that these reactions occurs at different sites, an observation that fits with both of the potential explanations discussed here.

D. Side-Path Donors: Which Side of the Reaction Center?

The arguments associated with this question are complex and have swung back and forth as new observations were made. The key observations in favor of the involvement of D1 are as follows: (i) A change in the ligand to Chl Z_{D1} results in a spectroscopic change associated with side-path donation while no such effect was seen when Chl Z_{D2} was mutated (Stewart et al., 1998). (ii) EPR measurements give a distance from Q_A to Chl Z that is compatible only with Chl Z being on the D1 side (Kawamori et al., 2002). The key observations in favor of the involvement of the D2 side are as follows: (i) A change in the ligand to Chl Z_{D2} results in spectroscopic changes associated with side path donation (Wang et al., 2003). (ii) EPR distance measurements from $Y_D^{\bullet}$ to Chl Z indicate that Chl Z is on the D2 side (Shigemori et al., 1998). (iii)The Cyt b_{559} is only on the D2-side (Zouni et al., 2001). (iv) The carotene is only on the D2 side (Kamiya and Shen, 2003; Ferreira et al., 2004).

The early debate between the proponents of either the D1-side or the D2-side was tilted strongly in the direction of D2, when the crystal structure showed that Cyt b_{559} was on the D2 side. The proponents of the D1-side then favored a 'both sides' model, putting their faith in a symmetrical reaction center, and encouraged by spectroscopic features that could be interpreted indicating two Chl Zs and two Car cations (Tracewell et al., 2001a,b; Telfer et al., 2003; Tracewell and Brudvig, 2003). The idea was put forward that symmetrical carotenoids could be present, allowing the positive charge to equilibrate between both carotenoids and both Chl Zs (Tracewell et al., 2001a,b; Tracewell and Brudvig, 2003). The absence of a D1 Car contradicts this model (Kamiya and Shen, 2003; Ferreira et al., 2004).

A novel solution was proposed to explain the involvement of Chl Z_{D1} when faced with the absence of a D1 Car. An electron transfer link was suggested through a series of Chls in CP 43, allowing the $Car_{D2}^{+\bullet}$ to oxidize the Chl Z_{D1} (Vasil'ev et al., 2003). This 'long-way-around' model was based on the poorly resolved crystal structure by Kamya and Shen (2003). In this model two carotenoids were proposed in D2, neither of which approached Chl Z_{D2}; thus it was implied that Chl Z_{D2} was not involved in the side-path. This model had a short life-time since Shen (2003) began revising his model of the carotenoids in 2003, only to be overtaken by a refined crystal structure (Ferreira et al., 2004). The 'long-way-around' model was dealt something of a double whammy by the following features of this structural model: (i) The Car_{D2} is close to Chl Z_{D2} making it rather likely that Chl Z_{D2} is involved in side-path electron transfer reactions. (ii) Even though an updated 'long way around' model can be defined (in which the Car_{D2} to $Car_{D2\text{-}43}$ gap is 3.8 Å, $Car_{D2\text{-}43}$ connects to the lumenal-side layer of CP43 Chls, and the CP43 Chls are, as expected for antenna pigments, in relatively close contact), the key CP43 Chl in the structure of Kamiya and Shen (2003), the Chl that triggered the original 'long way around' model, is absent in the structure of Ferreira

et al. (2004), leaving the nearest CP43 Chl to Chl Z_{D1} at a distance of 13 Å. These arguments do not argue strongly against the 'long way around' model nor the involvement of Chl Z_{D1}, they just make it less attractive.

Overall, the experimental data argue strongly for a D2-side path involving Car_{D2} as a donor to $P^{+\bullet}$, followed by electron donation from Cyt b_{559} to the $Car^{+\bullet}$ and finally slow electron donation from Q_BH_2 or PQH_2 to oxidized Cyt b_{559}. The involvement of Chl Z is much less clear. The proximity of Chl Z_{D2} to Car_{D2} indicates that electron transfer would be rapid, fitting with reports of partial Chl $Z^{+\bullet}$ formation at very low temperatures. The localization of the charge on Chl Z at higher temperatures indicates a lower redox potential than Car, but this may be more marked in isolated complexes, in which the peripheral position of both the Chl Z molecules and the carotenes could make them susceptible to solvent or detergent induced changes. A redox role for Chl Z_{D2} seems likely. The involvement of Chl Z_{D1}, is less clear and further experiments are required to determine the nature of its involvement in side path electron transfer.

V. Function of the Alternative Electron Transfer Pathway

A. A Protective Cycle for Redox Quenching of the Primary Electron Donor Cation

Many different functions for Cyt b_{559} have been suggested and these are dealt with in some detail elsewhere (Stewart and Brudvig, 1998). Here however we shall only discuss those associated with the function of the electron transfer side-pathway. Perhaps the most commonly held view for the existence of the side pathway focuses on the perceived necessity to provide electrons to $P^{+\bullet}$ in order to prevent it doing oxidative damage to the surrounding protein and neighboring chromophores. The idea is that whenever $P^{+\bullet}$ is sufficiently long-lived, the side-path can donate and thereby prevent unspecific oxidation reactions in the reaction center. This idea was proposed when the simple linear Cyt b_{559} to Chl Z to P pathway was considered to exist (Thompson and Brudvig, 1988) but it remains as valid for the more recently proposed branched pathway with Car as the branch point (Hanley et al., 1999). This begs the question whether this pathway can donate efficiently enough to provide an advantage to the organism.

The big question then is this: What is the rate of electron donation from Car to $P^{+\bullet}$ at room temperature? In D1/D2/Cyt b_{559} particles this rate was measured as the formation of the $Car^{+\bullet}$ at 980 nm and was found to be around 1 ms (Telfer et al., 1991). In more intact systems the measured rates vary but what is seen at all temperatures measured is that the yield for $Car^{+\bullet}$ formation is small and its apparent rate is the same as the lifetime of P^+ (R. Edge, P. Faller, K. Brettel, W. Leibl and A.W. Rutherford, unpublished). This implies that the real rate is significantly slower than the apparent rate. We attempted to optimize the rate and yield of $Car^{+\bullet}$ formation by removal of the Mn cluster, and then slowing the Y_Z donation rate by lowering the pH. Under these conditions the $P^{+\bullet}$ decay rate is dominated by slow Y_Z donation to $P^{+\bullet}$ or by $P^{+\bullet}/Q_A^{-\bullet}$ recombination. Even under these conditions the yield of $Car^{+\bullet}$ formation was low and its rate was equivalent to $P^{+\bullet}$decay. This suggests that the donation rate is slow even compared to $P^+/{}^{\bullet}Q_A^{-\bullet}$ recombination (200 μs) and from the yield of $Car^{+\bullet}$ formation we could estimate the rate to be in the region of 2 ms, similar to that reported in D1/D2/Cyt b_{559} particles (Telfer et al., 1991). We must conclude that even under the most extreme conditions, the efficiency of electron donation from the side pathway is low. These results indicate that the side-path can play at best a minor photoprotective role by electron donation to $P^{+\bullet}$. This conclusion based on work done at physiological temperature is backed up by the low temperature studies. The original work from de Paula et al. (1985) and Thompson and Brudvig (1988) that led to the suggestion that the side-path competed effectively with Y_Z donation as the temperature was lowered, led to the expectation that the two donation rates were similar at the cross-over temperature (approx 140K). As discussed above, this now appears to be incorrect and even at this temperature electron donation is slow (Schlodder and Derr, 2000; P. Faller and A.W. Rutherford, unpublished), competing poorly with the $P^{+\bullet}/Q_A^{-\bullet}$ reaction and the side-path is oxidized as a result of low quantum yield photo-accumulation.

The room temperature studies on Car were done under conditions where the Cyt b_{559} was pre-oxidized. Such studies starting with it in its reduced form, and measuring its yield per flash should reflect the efficiency of the side-path electron donation to $P^{+\bullet}$. Using this approach Buser et al. (1992) showed low yields in both intact and Mn-depleted PS II. Furthermore the rate of Cyt b_{559} oxidation was found to be close to that of lifetime of the final radical pair: $S_2Q_A^{-\bullet}$ and

$Y_Z^{\bullet}Q_A^{-\bullet}$ respectively. This is interpreted as showing that Cyt b_{559} reduction occurs as a result of an equilibrium between all the potential electron donors. Thus, the rate of electron donation from the side-pathway must be very slow even when the Cyt b_{559} is reduced prior to illumination.

There are no direct measurements of Chl Z formation in the literature. This is because absorption changes associated with its oxidation overlap with those of $P^{+\bullet}$, and while $P^{+\bullet}$ is formed with a quantum yield of 1, that of Chl Z is expected to be around two orders of magnitude smaller at most.

Hillman and Schlodder (1997) studied the $P^{+\bullet}$ formation and decay at low temperature in Mn-depleted PS II. The chemistry is dominated by $P^{+\bullet}/Q_A^{-\bullet}$ recombination but every time the side pathway donates an electron, $Q_A^{-\bullet}$ is trapped and the size of the $P^{+\bullet}$ signal is decreased on the subsequent flash. Measurement of the flash-induced decrease in the $P^{+\bullet}$ signal provides a measure of the yield and therefore the rate of electron donation from the side-pathway ($t_{½}$ of ~15 ms for Cyt b_{559} and 25 ms for Car donation to $P^{+\bullet}$ (Faller et al., 2001a).

Despite the very large optical change arising from $Car^{+\bullet}$, it has not been detected as a kinetic intermediate in oxidized Cyt b_{559} formation. It thus appears that electron donation from Cyt b_{559} to $Car^{+\bullet}$ is much faster than electron donation from Car to $P^{+\bullet}$. The current crystallographic model corresponds with this situation, with a much closer distance between Cyt b_{559} and Car_{D2} (12 Å) compared to Car to $P^{+\bullet}$(23 Å) (n.b., above we argued for a route, $Car_{D2} \rightarrow Chl_{D2} \rightarrow P$, where the distance for the first step is 13.1 Å and where the location of the cation on Chl_{D2} occurs through an equilibrium which greatly favors $P^{+\bullet}$), resulting in much faster electron transfer between Cyt b_{559} and Car_{D2}.

For the Chl $Z \rightarrow Car^{+\bullet}$ electron transfer, no data are yet available. The new crystal structure model with Car_{D2} approaching Chl Z_{D2} to a distance of 7.4 Å (Ferreira et al., 2004) indicates that electron transfer from Chl Z_{D2} to $Car_{D2}^{+\bullet}$ could in principle be rapid (tens of ps). So here again electron donation from Car to $P^{+\bullet}$ is the rate limiting step in the side-pathway. Furthermore, as we argued above, any involvement from Chl Z_{D1}, should it occur, is likely to be even slower that the rate of Car_{D2} oxidation by $P^{+\bullet}$. All of the above data indicate that electron donation from the side-path is too slow and inefficient to act as a significant protective pathway.

B. A Redox Mechanism for the Generation of a Fluorescence Quencher

A second mechanism has been proposed based on the fact that Chl $Z^{+\bullet}$ is a very effective quencher of PS II (Schweitzer and Brudvig, 1997). This arises from the broad absorption of Chl cation in the near infra-red, with a broad maximum around 820 nm. The idea is that the side pathway donates electrons at a low efficiency to $P^{+\bullet}$ and under most circumstances the electron comes from Cyt b_{559} which is in turn reduced slowly by PQH_2, perhaps through the Q_B site. However under certain conditions, (such as under conditions of stress), the side-path electron donation to $P^{+\bullet}$ outruns Cyt b_{559}^{ox} reduction. This could result from inefficiencies in the normal electron donation pathway (during photo-activation or inhibition of the Mn cluster) or whenever Cyt b_{559}^{ox} reduction is slow or does not occur (e.g., due to a shift to a low potential redox form). This would result in formation of the Chl $Z^{+\bullet}$. The quenching could dissipate energy and thus would help protect the reaction center from photodamage. One might expect that the lifetime of the Chl $Z^{+\bullet}$ quencher would be limited by an electron from the quinone complex arriving on the pre-oxidized Cyt b_{559}.

Again this basic idea of Chl $Z^{+\bullet}$ acting as a protective quencher was suggested when the linear Cyt $b_{559} \rightarrow$ Chl $Z \rightarrow P^{+\bullet}$ pathway was under consideration, however the realization that Car is involved as a branch point did not change the validity of the idea. The additional possibility exists that the $Car^{+\bullet}$ itself may also be a quencher (Hanley et al., 1999) and indeed may contribute to the quenching effect attributed to Chl $Z^{+\bullet}$, especially if their potentials are relatively close. The main question concerning the validity of this model is whether Chl $Z^{+\bullet}$ has a lifetime that is long enough at room temperature to allow it to play a useful quenching role. There have been several reports of quenching states generated in PS II under various (mainly detrimentally strong light) conditions. It remains possible that these correspond to long-lived Chl $Z^{+\bullet}$ states. The specific link between such states and Chl $Z^{+\bullet}$ has yet to be demonstrated however.

It is worth pointing out that a role for Chl $Z^{+\bullet}$ as a protective fluorescence quencher would correspond to situation in which the redox potential of the Chl was significantly lower than the neighboring species (particularly the carotene and other Chls). In this way the charge would localize on the Chl Z and not wander around the reaction center leading to

potentially undesirable chemistry. Thus we consider that this role is not particularly compatible with the equal potential equilibrium model recently proposed by Tracewell et al. (2003).

C. A New Perspective: A Protective Cycle for Redox Quenching of the β-Carotene Cation Radical

Photodamage can occur due to the formation of triplet Chl (^{3}Chl) either from excited Chl singlet through inter-system crossing or through radical pair recombination (Rutherford and Krieger-Liskay, 2001; Chapters 23 and 27) . The latter mechanism occurs within photosynthetic reaction centers. ^{3}Chl reacts readily with O_2 generating singlet oxygen, $^1O_2$, a very potent oxidant that can kill the organism. The protection provided by the carotenoids is achieved through a close association between the carotenoids and Chl which leads to a quenching of the Chl triplet. Moreover, carotenoids are also known to quench singlet oxygen directly (Cogdell and Frank, 1987; Chapters 23 and 27).

Radical pair recombination Chl triplet is thought to be an important source of photodamage in PS II (Rutherford and Krieger-Liskay, 2001; Chapter 27, Chow and Aro). In BRCs a carotenoid is located close to the primary electron donor, $P^{+\bullet}$, on the inactive branch of the reaction center, the equivalent of the D2-side in PS II, and quenches the Chl triplet generated by radical pair recombination (Cogdell and Frank, 1987).

While an equivalent role for carotenoid sounds like a particularly good idea in PS II, especially since it is by its nature in an O_2-rich environment and its Chl triplet state is at a higher energy and thus even more ready to generate singlet oxygen, there is no evidence that the carotenoid is able to quench Chl triplet either in D1/D2/Cyt b_{559} particles (Takahashi et al., 1987) or in more intact PS II (Hillmann et al., 1995; Van Mieghem et al., 1995). A likely explanation for this is that, unlike $P^{+\bullet}$ in the BRC, $P^{+\bullet}$ in PS II is so oxidizing that it would be able to oxidize carotenoid in competition with the Y_Z thus decreasing the efficiency of water oxidation (Telfer, 2002). On the other hand, there is indirect evidence that the β-carotenes in PS II do play a role in scavenging singlet oxygen (Telfer et al., 1994).

Thinking along these lines it is possible to rationalize the existence of the side-path electron transfer chain. It is simply a result of two features of PS II: (i) the very high redox potential of $P^{+\bullet}$, which means that any near by component will be oxidized; and (ii) the requirement for carotenoid to be at the center of the reaction center so that it can play a protective role as a singlet oxygen quencher. The Car thus occupies a compromise position: it is close enough to the core Chls to allow singlet oxygen to be quenched close to its site of generation but at this distance it cannot avoid a very low quantum yield of oxidation by $P^{+\bullet}$. Thus we see that the donation pathway from Cyt b_{559} is there to remove the highly oxidative $Car^{+\bullet}$ in order to prevent non-specific damage and to return it to its active, $^1O_2$ quenching form. The reduction of Cyt b_{559} with electrons from the reducing side of PS II restores it to its reduced form, primed to quench $Car^{+\bullet}$ whenever it is generated with a low quantum yield. This then fits with the idea that electron transfer is much more efficient from Cyt b_{559} to $Car^{+\bullet}$ than for Car to $P^{+\bullet}$. Because of the large number of photochemical events occurring in PS II and the periods in the lifetime of the enzyme when water oxidation does not occur (e.g., prior to assembly of the Mn cluster), Car oxidation is predicted to be inevitable.

The redox quenching role for Cyt b_{559} could be its main function. However, the variable redox potential of the cytochrome remains unexplained. One can dip into the many suggestions in the literature (reviewed in Stewart and Brudvig, 1998) looking for an explanation but that suggested by Schweitzer and Brudvig (1997), i.e., that the cytochrome redox state controls the production of the fluorescence quencher Chl $Z^{+\bullet}$, as described above, is the most appropriate for the present discussion since it relates to the side-path electron donors. This aspect of the function of the side-path can be painlessly incorporated into our new model. However it is not yet clear if Chl $Z^{+\bullet}$ acts as a quencher under physiologically relevant conditions. Most studies indicate that it is short-lived but there is little information about the fate of Chl $Z^{+\bullet}$ and its reaction partners[1].

[1] The first observations of $Car^{+\bullet}$ formation in PS II were made when a range of chemicals reagents were added to the sample. These chemicals fall under the definition of 'ADRY' reagents as defined by Renger (1973) in that they accelerate the deactivation of the OEC and include FCCP, ANT2P, tetraphenol boron and phenolic herbicides. While their function is not wholly clear, extending earlier thinking (Renger, 1973; Ghanotakis et al., 1982) in the context of the side-pathway, we consider that they work as high potential electron donors to any species within the lipophilic environment that has a potential high enough to oxidize the ADRY reagent. Potentially this could include the Mn cluster in the S_2 and S_3 state, the tyrosyl radicals and P^+. It seems that after donating an electron to PS II, the oxidized ADRY reagent remains rapidly diffusible in the lipophilic environment. When it encounters an

VII. Conclusions

The side pathway of electron donors in PS II is made up of a branched pathway in which the Car on D2 donates to $P^{+\bullet}$ and the $Car^{+\bullet}$ formed is rapidly reduced by Cyt b_{559}, or by Chl Z should the cytochrome be pre-oxidized. The electron donation from Car to $P^{+\bullet}$ is slow and works at a very low quantum yield. It is suggested that this reaction has evolved to be as slow as possible in order to minimize competition with water oxidation. The fact that it occurs at all may be due to the need for Car to be in the heart of the reaction center, close to the source of singlet O_2 generation (i.e., the radical pair recombination Chl triplet). The quenching of singlet O_2 is proposed to be the principal role of Car but in fulfilling this role it is inevitably at risk of being oxidized by $P^{+\bullet}$. When this rare but inevitable event occurs it is the role of the Cyt b_{559} to return $Car^{+\bullet}$ to its active unoxidized form, at the same time preventing potentially damaging reactions caused by $Car^{+\bullet}$. The cycle is completed when the oxidized Cyt b_{559} is reduced by electrons from the plastoquinone pool, possibly through the Q_B site.

Thus we suggest that the side-pathway of electron transfer in PS II plays a protective role aimed at maintaining Car in its active, unoxidized form. The role of Chl Z may be to act as a fluorescence quencher and hence energy trap, when oxidized by $Car^{+\bullet}$, a reaction that only occurs when Cyt b_{559} is already oxidized. The redox state of the Cyt b_{559} thus would regulate this quencher. Many questions remain, particularly the identity of Chl Z and the role of Chl Z on the D1 side, and the possibilities remain open that the cation equilibrates between Car_{D2} and Chl Z_{D2}, between Car_{D2} and the $Car_{D2\text{-}43}$, and between Car_{D2} and Chl Z_{D1} via $Car_{D2\text{-}43}$ and a several Chls of CP43 . Doubtless, some of these ambiguities will be resolved with further experimentation focusing on identifying the carotenoids and Chls that bear the cation under different conditions.

oxidizable species it extracts an electron from it returning to its active state as a donor ready to donate to another reaction center, hence the ability of these reagents to work in sub-stoichiometric concentrations. In this model Cyt b_{559} can be oxidized by ADRY reagents, possibly due to the reagent itself being oxidized by $Y_D^{+\bullet}$ in a dark-adapted system. Carotenoid cations are much less stable so their formation is observed only transiently immediately after the flash illumination. It seems quite possible that carotenoids other than those in the D2 part of the reaction center are oxidized when lipophilic anions are present in the sample. Indeed we have observed that the amplitude of carotenoid cation generated per flash at room temperature in the presence of tetraphenol boron is found to be smaller in PS II preparations with smaller antenna implying that the oxidized reagent is able to react with carotenoids in the antenna (R. Edge and A.W. Rutherford, unpublished).

Acknowledgments

We thank Drs. Tony Mattioli, Sun Un, Ruth Edge, Charilaos Goussias, Anabella Ivancich, Yiannis Deligiannakis, Jonathan Hanley, Alain Boussac, Klaus Brettel, Paul Mathis, Andy Pascal and Bruno Robert (CEA Saclay), Anja Liszkay (University of Freiburg, Germany), Fabrice Rappaport (IBPC, Paris) Richard J. Debus (UC Riverside), Thorsten Maly, Fraser MacMillan (University of Frankfurt), Gary Brudvig (Yale), Alison Telfer (London) and Bruce Diner (DuPont) for helpful discussion. P.F. was supported by a grant from the Swiss National Science Foundation and C.F. was a Marie Curie Training Site studentship supported by the EU.

References

Bialek-Bylka GE, Tomo T, Satoh K and Koyama Y (1995) 15-*cis*-beta-carotene found in the reaction center of spinach Photosystem II. FEBS Lett 363 : 137–140

Bratt PJ, Poluektov, OG, Thurnauer MC, Krzystek J, Brunel L-C, Schrier J, Hsiao Y-W, Zerner M and Angerhofer A (2000) The *g*-factor anisotropy of plant chlorophyll a^+. J Phys Chem B 104: 6973–6977

Breton J, Duranton J and Satoh K (1988) Orientation of pigments in the reaction center and the core antenna of Photosystem II. In: Scheer H and Schneider S (eds) Photosynthetic Light-Harvesting Systems: Organization and Function, pp 375–386. Walter de Gruyter, Berlin

Buser CA, Diner BA and Brudvig GW (1992) Photooxidation of cytochrome *b*559 in oxygen-evolving Photosystem II. Biochemistry 31:11449–11459

Cogdell RJ and Frank HA (1987) How carotenoids function in photosynthetic bacteria? Biochim Biophys Acta 895: 63–79

Cua A, Stewart DH, Brudvig GW and Bocian DF (1998) Selective resonance Raman scattering from chlorophyll Z in Photosystem II via excitation into near-infrared absorption band of the cation. J Am Chem Soc 120: 4532–4533

Dawe EA and Land EJ (1975) Radical ions derived from photosynthetic polyenes. J Chem Soc Faraday Trans 1, 71 : 2162–2169

De Paula JC, Innes JB and Brudvig GW (1985) Electron transfer in Photosystem II at cryogenic temperatures. Biochemistry 24: 8114–8120

Deligiannakis Y, Hanley J and Rutherford AW (2000) Carotenoid oxidation in Photosystem II: 1D and 2D ESEEM study. J Am Chem Soc 122: 400–401

Diner BA, Schlodder E, Nixon PJ, Coleman WJ, Rappaport F, Lavergne J, Vermaas WFJ and Chrisholm DA (2001) Site-di-

rected mutations at D1-His198 and D2-His197 of Photosystem II in *Synechocystis* PCC 6803: Sites of primary charge separation and cation and triplet stabilization. Biochemistry 40: 9265–9281

Edge R, Land EJ, McGarvey DJ, Burke M and Truscott TG (2000) The reduction potential of the β-carotene+/β-carotene couple in an aqueous micro-heterogeneous environment. FEBS Lett 471:125–127

Faller P, Rutherford AW and Un S (2000) High-field EPR study of carotenoid and the angular orientation of chlorophyll-z in Photosystem II. J Phys Chem B 104: 10960–10963

Faller P, Pascal A and Rutherford AW (2001a) β-Carotene redox-reaction in Photosystem II: Electron transfer pathway. Biochemistry 40: 6431–6440

Faller P, Maly T, Rutherford AW and MacMillan F (2001b) Chlorophyll and carotenoid radicals in Photosystem II studied by pulsed ENDOR. Biochemistry 40: 320–326

Ferreira KN, Iverson TM, Maghlaoui K, Barber J and Iwata S (2004) The architecture of the oxygen evolving enzyme. Science 303: 1831–1838

Frese RN, Germano M, de Weerd FL, van Stokkum, AY, Shuvalov VA, van Gorkom HJ and Dekker JP (2003) Electric field effects on the chlorophylls, pheophytins and beta carotenes in the reaction centre of Photosystem II. Biochemistry 42: 9205–9213

Germano M, Shkuropatov AJ, Permentier H, de Wijn R, Hoff AJ, Shuvalov VA and van Gorkom HJ (2001) Pigment organization and their interactions in reaction centers of Photosystem II: Optical spectroscopy at 6 K of reaction centers with modified pheophytin composition. Biochemistry 40: 11472–11482

Ghanotakis D.F., Yerkes, C.T. and Babcock G. T. (1982) The role of reagents accelerating the deactivation reactions of the water splitting enzyme. Biochim Biophys Acta 682: 21–31

Grant JL, Kramer VJ, Ding R and Kispert LD (1988) Carotenoid cation radicals: electrochemical, optical, and EPR study. J Am Chem Soc 110: 2151–2157

Goussias H, Boussac A and Rutherford AW (2002) Photosystem II and photosynthetic oxidation of water: An overview. Philos Trans Roy Soc Lond B Biol Sci 357: 1369–1381

Hanley J, Deligiannakis Y, Pascal A, Faller P and Rutherford AW (1999) Carotenoid oxidation in Photosystem II. Biochemistry 38: 8189–8195

Hillmann B and Schlodder E (1997) Electron transfer reactions in Photosystem II core complexes from *Synechococcus* at low temperature-difference spectrum of P680+Qa-/p680 Qa at 77K. Biochim Biophys Acta 1231: 76–88

Hillmann B, Brettel K, van Mieghem F, Kamlowski A, Rutherford AW and Schlodder E (1995) Charge recombination reactions in Photosystem II. 2. Transient absorbance difference spectra and their temperature dependence. Biochemistry 34 : 4814–4827

Himo F (2001) Density functional theory study of the β-carotene radical cation. J Phys Chem A 105: 7933–7937

Jeevarajan AS, Kispert L D and Piekara-Sady L (1993) An ENDOR study of carotenoid cation radicals on silica-alumina solid supports. Chem Phys Lett 209: 269–274

Jeevarajan JA, Wei CC, Jeevarajan AS and Kispert LD (1996a) Optical absorption spectra of dications of carotenoids. J Phys Chem 100: 5637–5641

Jeevarajan AS, Kispert LD, Chumanov G, Zhou C and Cotton TM (1996a) Resonance Raman study of carotenoid cation radicals. Chem Phys Lett 259: 515–522

Johnson G, Rutherford AW and Krieger A (1995) A change in the midpoint potential of QA in Photosystem II associated with photo-acrtivation of oxygen evolution. Biochim Biophys Acta 1229: 202–207

Kamiya N and Shen JR (2003) Crystal structure of oxygen-evolving Photosystem II from *Thermosynechococcus vulcanus* at 3.7-Å resolution. Proc Natl Acad Sci USA 100: 98–103

Kawamori A, Katsuta N and Hara H (2002) Structural analysis of three-spin systems of Photosystem II by PELDOR. Appl Magn Reson 23: 557–569

Konovalova TA, Krzystek J, Bratt PJ, van Tol J, Brunel L-C and Kispert LD (1999) 95–670 GHz EPR studies of canthaxanthin radical cation stabilized on a silica-alumina surface. J Phys Chem B 103: 5782–5786

Konovalova TA, Dikanov SA, Bowman MK and Kispert LD (2001) Detection of anisotropic hyperfine components of chemically prepared carotenoid radical cations: 1D and 2D ESEEM and pulsed ENDOR study. J Phys Chem B 105: 8361–8368

Koulougliotis D, Innes JB and Brudvig GW (1994) Localization of chlorophyll z in Photosystem II. Biochemistry 33:11814–11822

Knaff DB and Arnon DI (1969) Light-induced oxidation of a chloroplast *b*-type cytochrome at –189 °C. Proc Natl Acad Sci USA 63: 963–969

Kwa SLS, Newell WR, van Grondelle R and Dekker JP (1992) The reaction center of Photosystem II studied by polarized fluorescence spectroscopy. Biochim Biophys Acta 1099: 193–202

Lakshmi KV, Reifler MJ, Brudvig GW, Poluektov OG, Wagner AM and Thurnauer MC (2000) High-field EPR study of carotenoid and chlorophyll cation radicals in Photosystem II. J Phys Chem B 104: 10445–10448

Lakshmi KV, Poluektov OG, Reifler MJ, Wagner AM, Thurnauer MC and Brudvig GW (2003) Pulsed high frequency EPR study on the location of carotenoid and chlorophyll cation radicals in Photosystem II. J Am Chem Soc 125: 5005–5014

Lubitz W (1991) EPR and ENDOR studies of chlorophyll cation and anion radicals. In: Scheer H (ed) Chlorophylls, pp 903–944. CRC Press, Boca Raton

MacMillan F, Rohrer M, Krzystek J, Brunel L-C and Rutherford AW (1998) A high-field/high frequency EPR characterization of the primary donor (P^+) in bacterial and plant photosynthetic reaction centers. In: Garab G (ed) Photosynthesis: Mechanism and Effects, Vol 2, pp 715–718. Kluwer Academic Publishers, Dordrecht

Mathis P and Vermeglio A (1972) Transient forms of carotenoids. Triplet state and radical cation. Photochem Photobiol 15 : 157–164

Mathis P and Vermeglio A (1975) Chlorophyll radical cation in Photosystem II of chloroplasts. Millisecond decay at low temperature. Biochim Biophys Acta 369 : 371–381

Michel H and Deisenhofer J (1988) Relevance of the photosynthetic reaction center from purple bacteria to the structure of Photosystem II. Biochemistry 27: 1–7

Moore TA, Gust D, Mathis P, Mialocq J-C, Chachaty C, Bensasson RV, Land EJ, Doizi D, Liddell PA, Lehman WR, Nemethy GA and Moore AL (1984) Photo-driven charge separation in a carotenoporphyrinquinone triad. Nature 307: 630–632

Nanba O and Satoh K (1987) Isolation of a Photosystem II reaction center consisting of D-1 and D2 polypeptides and cytochrome *b*-559. Proc Natl Acad Sci USA 84: 109–112

Noguchi T and Inoue Y (1995) Molecular interactions of the redox-active accessory chlorophyll on the electron donor side

of Photosystem II as studied by Fourier transform infrared spectroscopy. FEBS Lett 370: 241–244

Noguchi T, Mitsuka T and Inoue Y (1994) Fourier transform infrared spectrum of the radical cation of β-carotene photoinduced in Photosystem II. FEBS Lett 356: 179–182

Nugent JHA, Muhiuddin IP and Evans MCW (2002) Electron transfer from the water oxidizing complex at cryogenic temperatures. Biochemistry 41: 4117–4126

Page CC, Moser CC, Chen X and Dutton PL (1999) Natural engineering principles of electron tunneling in biological oxidation-reduction. Nature 402: 47–52

Pascal A, Telfer A, Barber J and Robert B (1999) Fourier-transform resonance Raman spectra of cation carotenoid in Photosystem II reaction centres. FEBS Lett 453: 11–14

Rappaport F and Diner BA (2002) Structure, dynamics, and energetics of the primary photochemistry of Photosystem II of oxygenic photosynthesis. Annu Rev Plant Biol 53 : 551–580

Renge I, van Grondelle R and Dekker JP (1996) Matrix and temperature effects on absorption spectra of β-carotene and pheophytin in solution and in green plant Photosystem II. J Photochem Photobiol A 96: 109–121

Renger G (1973) Studies on the mechanism of destabilization of the positive charges trapped in the photosynthetic water splitting enzyme system Y by a deactivation-accelerating agent. Biochim Biophys Acta 314: 390–402 314

Rhee K-H (1998) Three-dimensional structure of Photosystem II reaction center by electron cryo-microscopy. PhD Thesis. Univ Heidelberg, Heidelberg

Rigby SEJ, Nugent JHA and O'Malley PJ (1994) ENDOR and special triple resonance studies of chlorophyll cation radicals in photosystem 2. Biochemistry 33: 10043–10050

Ruffle SV, Donnelly D, Blundell T and Nugent JHA (1992) A three-dimensional model of the Photosystem II reaction center of *Pisum sativum.* Photosynth Res 34: 287–300

Rutherford AW and Faller P (2001) The heart of Photosystem II in glorious 3D. Trends Biochem Sci 26: 341–344

Rutherford AW and Faller P (2002) Photosystem II: evolutionary perspectives. Philos Trans Roy Soc Lond B Biol Sci 358: 245–253

Rutherford AW and Krieger-Liskay A (2001) Herbicide induced oxidative stress in Photosystem II. Trends Biochem Sci 26: 648–653

Satoh K (1996) Introduction to the Photosystem II reaction center — Isolation and biochemical and biophysical characterization. In: Ort DR and Yocum CF (eds) Oxygenic Photosynthesis: The Light Reactions, pp 193- 211. Kluwer Academic Publishers, Dordrecht

Schenck CC, Diner B, Mathis P and Satoh K (1982) Flash-induced carotenoid radical formation in Photosystem II. Biochim Biophys Acta 680: 216–227

Schweitzer RH and Brudvig GW (1997) Fluorescence quenching by chlorophyll cations in Photosystem II. Biochemistry 36: 11351–11359

Shen JR and Kamiya N (2003) Functions of carotenoids and other pigments in Photosystem II from a structural point of view. (Abstract 425) European Photobiological Society Meeting, Vienna

Shigemori K, Hara H, Kawamori A and Akabori K (1998) Determination of distances from tyrosine D to QA and chlorophyll Z in Photosystem II studied by '2+1' pulsed EPR. Biochim Biophys Acta 1363: 187–198

Stewart DH and Brudvig GW (1998) Cytochrome *b*559 of Photosystem II. Biochim Biophys Acta 1367: 63–87

Stewart DH, Cua A, Chisholm DA, Diner BA, Bocian DF, Brudvig GW (1998) Identification of histidine 118 in the D1 polypeptide of Photosystem II as the axial ligand to chlorophyll Z. Biochemistry 37:10040–10046

Takahashi Y, Hansson O, Mathis P and Satoh K (1987) Primary radical pair in the Photosystem II reaction center. Biochim Biophys Acta 893: 49–59

Telfer A (2002) What is β-carotene doing in the photosystem two reaction centre? Philos Trans Roy Soc Lond B 357:1431–1439

Telfer A, De Las Rivas J and Barber J (1991) β-Carotene within the isolated Photosystem II reaction centre: photooxidation and irreversible bleaching of this chromophore by oxidized P680. Biochim Biophys Acta 1060: 106 –114

Telfer A, Dhami S, Bishop SM, Phillips D and Barber J (1994) β-Carotene quenches singlet oxygen formed by isolated Photosystem II reaction centers. Biochemistry 33: 14469–14474

Telfer A, Frolov D, Barber J, Robert B and Pascal A (2003) Oxidation of the two beta-carotene molecules in the Photosystem II reaction center. Biochemistry 42:1008–1015

Thompson LK and Brudvig GW (1988) Cytochrome *b*-559 may function to protect Photosystem II from photoinhibition. Biochemistry 27:6653–6658

Tomo T, Mimuro M, Iwaki M, Kobayashi M, Itoh S and Satoh K (1997) Topology of pigments in the isolated Photosystem II reaction center studied by selective extraction. Biochim Biophys Acta 1321: 21–30

Tracewell CA and Brudvig GW (2003) Two redox active beta-carotene molecules in Photosystem II. Biochemistry 42: 9127–9136

Tracewell CA, Cua A, Stewart D, Bocian DF and Brudvig GW (2001a) Characterization of carotenoid and chlorophyll photooxidation in Photosystem II. Biochemistry 40: 193–203

Tracewell CA, Vrettos JS, Bautista JA, Frank HA and Brudvig GW (2001b) Carotenoid photooxidation in Photosystem II. Arch Biochem Biophys 365:61–69

Un S, Dorlet P and Rutherford AW (2001) A high-field EPR tour of radicals in Photosystem I and II. Appl Magn Reson 21: 341–361

Van Dorssen RJ, Breton J, Plijter JJ, Satoh K, van Gorkom HJ and Amesz J (1987a) Spectrocopical properties of the reaction center and of the 47kDa chlorophyll protein of Photosystem II. Biochim Biophys Acta 893: 267–274

Van Dorssen RJ, Plijter JJ, Dekker JP, den Ouden A, Amesz J. and van Gorkom HJ (1987b) Spectroscopic properties of chloroplast grana membranes and the core of Photosystem II. Biochim Biophys Acta 890: 134–143

Van Mieghem F, Brettel K, Hillmann B, Kamlowski A, Rutherford AW and Schlodder E (1995) Charge recombination reactions in Photosystem II. I. Yields, recombination pathways, and kinetics of the primary pair. Biochemistry 34: 4798–4813

Vasil'ev S, Brudvig GW and Bruce D (2003) The X-ray structure of Photosystem II reveals a novel electron transport pathway between P680, cytochrome *b*559 and the energy-quenching cation, ChlZ+. FEBS Lett 543 : 159–163

Velthuys BR (1981) Carotenoid and cytochrome *b*559 reactions in Photosystem II in the presence of tetraphenylboron. FEBS Lett 126: 272–276

Visser JWM, Rijgersberg CP and Gast P (1977) Photooxidation

of chlorophyll in spinach chloroplasts between 10K and 180K. Biochim Biophys Acta 460: 36–46

Vrettos JS, Stewart DH, dePaula JC and Brudvig GW (1999) Low-temperature optical and resonance Raman of carotenoid cation radical in Photosystem II. J Phys Chem B 103: 6403–6406

Wang J, Gosztola D, Ruffle SV, Hemann C, Seibert M, Wasielewski MR, Hille R, Gustafson TL and Sayre RT (2002) Functional asymmetry of Photosystem II D1 and D2 peripheral chlorophyll mutants of *Chlamydomonas reinhardtii*. Proc Natl Acad Sci USA 99: 4091–4096

Whitmarsh J and Cramer WA (1977) Kinetics of the photoreduction of cytochrome *b*-559 by Photosystem II. Biochim Biophys Acta 460: 280–289

Yurela I, Tomas R, Sanjuan ML, Torrado E, Aured M and Picorel R (1998) The configuration of β-carotene in the Photosystem II reaction center. Photochem Photobiol 68: 729–737

Zhang C and Styring S (2003) Formation of split electron paramagnetic resonance signals in Photosystem II suggests that Tyrosine Z can be photoxidised at 5K in the S_0 and S_1 states of the oxygen evolving complex. Biochemistry 42: 8066–8076

Zhang C, Boussac A and Rutherford AW (2004) Low-temperature electron transfer in Photosystem II: A tyrosyl radical and semiquinone charge pair. Biochemistry 43: 13787–13795

Zouni A, Witt HT, Kern J, Fromme P, Krauss N, Saenger W and Orth P (2001) Crystal structure of Photosystem II from *Synechococcus elongatus* at 3.8 Å resolution. Nature 409: 739–743